Title: Characteristics of multiwalled carbon nanotubes-rhenium nanocomposites with varied rhenium mass fractions

Author: Anna D. Dobrzańska-Danikiewicz, Weronika Wolany, Dariusz Łukowiec, Karolina Jurkiewicz, Paweł Niedziałkowski

Citation style: Dobrzańska-Danikiewicz Anna D., Wolany Weronika, Łukowiec Dariusz, Jurkiewicz Karolina, Niedziałkowski Paweł. (2017). Characteristics of multiwalled carbon nanotubes-rhenium nanocomposites with varied rhenium mass fractions. " Nanomaterials and Nanotechnology" (Vol. 7, (2017), art. no. 1847980417707173, s. 1-8), doi 10.1177/1847980417707173

Research Article

NANOMATERIALS AND NANOTECHNOLOGY

Nanomaterials and Nanotechnology
Volume 7: 1–8

DOI: 10.1177/1847980417707173
journals.sagepub.com/home/nax
SAGE

Characteristics of multiwalled carbon nanotubes-rhenium nanocomposites with varied rhenium mass fractions

Anna D Dobrzańska-Danikiewicz[1], Weronika Wolany[1], Dariusz Łukowiec[1], Karolina Jurkiewicz[2], and Paweł Niedziałkowski[3]

Abstract

The purpose of the article is to discuss the process of oxidation of carbon nanotubes subsequently subjected to the process of decoration with rhenium nanoparticles. The influence of functionalization in an oxidizing medium is presented and the results of investigations using Raman spectroscopy and infrared spectroscopy are discussed. Multiwalled carbon nanotubes rhenium-type nanocomposites with the weight percentage of 10%, 20% and 30% of rhenium are also presented in the article. The structural components of such nanocomposites are carbon nanotubes decorated with rhenium nanoparticles. Microscopic examinations under transmission electron microscope and scanning transmission electron microscope using the bright and dark field confirm that nanocomposites containing about 20% of rhenium have the most homogenous structure.

Keywords

Nanocomposites, carbon nanotubes, rhenium, nanoparticles, TEM

Date received: 4 February 2016; accepted: 22 March 2017

Topic: Nanocomposites, Nanophase Materials and Nanoscale Characterizations
Topic Editor: Leander Tapfer

Introduction

The discovery of carbon nanotubes (CNTs), which were characterized in detail in 1991,[1] was a breakthrough in materials engineering. Singlewalled carbon nanotubes (SWCNTs) are cylindrical objects constructed from rolled single graphene layer. Multiwalled carbon nanotubes (MCWNTs) consist of co-axially rolled several graphene tubes. The excellent physiochemical properties of CNTs result from their characteristic structure formed by a honeycomb-shaped hexagonal graphene lattice in which carbon atoms with sp2 hybridization are forming six-membered rings.[1–5] The CNTs combine excellent electrical and optoelectrical properties, feature high chemical stability and an extended active surface, which makes them a suitable material for applications in many branches of industry[5–13] often using modern production organization systems.[14,15] Numerous publications exist confirming the effective application of nanocomposites composed of CNTs covered with metal nanoparticles, for different sensors, due to their ultra-high sensitivity, selectivity and a fast response rate of such systems.[16,17] The construction of catalysts of fuel cell components and application as a catalyst

[1] Faculty of Mechanical Engineering, Silesian University of Technology, Gliwice, Poland
[2] Silesian Center for Education and Interdisciplinary Research, University of Silesia, Chorzów, Poland
[3] Faculty of Chemistry, University of Gdańsk, Gdańsk, Poland

Corresponding author:
Weronika Wolany, Faculty of Mechanical Engineering, Silesian University of Technology, Konarskiego 18A St., 44-100 Gliwice, Poland.
Email: weronika.wolany@gmail.com

of diverse chemical reactions is an interesting use of such nanocomposites.[18–20] The authors have made an assumption that nanocomposites, whose structural components are CNTs decorated with rhenium (Re) nanoparticles, will be an interesting, modern material useful for various applications. Creation of MWCNTs-Re-type nanocomposites is an interesting research aspect, mainly due to relatively few publications concerning nanocomposites consist of carbon nanostructures and Re in form of nanoparticles. Re, being a group 7 element, has similar physical properties to group 6 metals, that is, molybdenum and wolfram. On the other hand, it exhibits characteristics typical to platinum group metals (platinum, ruthenium and osmium). Re is a heavy metal (density of 21.02 g/cm3), with its appearance similar to steel, having a very high melting point and boiling point of, respectively, 3180°C and 5600°C.[21,22] Excellent physiochemical properties make Re suitable for applications in the progressive industries. The space and aviation industry manufactures its products using alloys containing Re, including production of components of jet engines, turbine blades, thermal shields and combustion chambers. The production of thermoelements and heating elements, incandescent parts, cathodes and electron guns is an important field of applications for Re, which has lower volatility and higher resistance to high temperatures as compared to wolfram.[23–25] The radioactive isotopes 186Re and 188Re are employed in diagnostics and for destruction of tumorous cells.[26] The application areas of Re also include analytical chemistry and as a catalyst for the manufacture of high-octane fuels.[21,22,27]

The results which are presented in this article are continuation of research related to the production of MWCNTs – Re nanocomposites. The methodology has been first described by Dobrzańska-Danikiewicz et al.[28] The new aspect of this article is to present the diverse weight percentage of Re in MWCNTs-Re-type nanocomposites. This was one of the elements taken into account during optimization of fabrication method. The main criterions in this respect were the uniform distribution of Re nanoparticles on the surface of CNTs and no tendency to agglomerate. The structure of MWCNTs-Re-type nanocomposites was developed in relation to future practical applications, for example, gas or liquid sensors or as catalysts for selected chemical reactions.

Materials and methods

Synthesis of MWCNTs-Re nanocomposites

The MWCNTs fabricated by catalytic chemical vapour deposition on a silicon substrate containing a catalyst in the form of a thin film of iron, and two nanometric buffer layers of aluminium oxide and silicon oxide were applied for the fabrication of MWCNTs-Re nanocomposites with a different concentration of elements. C_2H_4 was used as a source of carbon and H_2 and argon (Ar) were used as other process gases. The CNTs synthesis process, described thoroughly in the earlier publications,[29,30] was carried out at 750°C for 45 min. Pristine MWCNTs, being an input material for nanocomposite fabrication, contained few impurities in the form of metallic catalyst and amorphous carbon nanoparticles. $HReO_4$ acid is a Re precursor.

The oxidization of CNTs using acids, their mixtures or other strongly oxidizing compounds is an effective method for functionalization and purification of CNTs.[31–37] The CNTs selected for the experiment were weighed, grouped into three equal portions and then subjected to a functionalization process with concentrated nitric acid (HNO_3), principally because such functionalization is effective. The process was carried out at room temperature for 5 h using ultrasounds. During the tests, it has been checked that the use of pure MWCNTs is less effective because Re nanoparticles detached from the outer walls of CNTs during further processing. The connection is not as stable as in the case of the use of oxidized MWCNTs.

A Re precursor (perrhenic acid – $HReO_4$) was added with a pipette to three portions of oxidized CNTs. The rate of components was determined to achieve nanocomposites with a weight percentage of, respectively, 10%, 20% and 30% of Re. A nanotubes impregnation process using ultrasounds was continued for 1 h. The wet nanotube materials were placed into quartz vessels at the next stage and were subjected to heating at 800°C for 45 min. Hydrogen was a reducing agent, and a protective atmosphere was created by using Ar. As assumed, during the reduction of metal precursor, the Re nanocrystals formed are attached automatically to the place where functional groups exist on the surface of CNTs. Permanent combination of the mentioned components is achieved as a result and an MWCNTs-Re-type nanocomposite was created (Figure 1).

Characterization techniques

Scanning electron microscopy (SEM) using SEM Supra 35 by Carl Zeiss and transmission electron microscopy (TEM) were employed to observe pristine CNTs. The samples before and after the functionalization process were analysed with the Raman spectroscopy technique with an InVia Renishaw Raman spectrometer by Renishaw, fitted with an ion and Ar laser with the wavelength of $\lambda = 514$ nm and power of 50 mW with a plasma filter for 514 nm. Infrared (IR) spectroscopy is a method complementary to Raman spectroscopy, because it can confirm the changes in the carbon network of nanotubes subjected to oxidation. The IR was used to determine which functional groups exist in the analysed sample containing oxidized CNTs, using an IFS66 infrared spectrometer from Bruker for this aim. The nanocomposite materials achieved were viewed using TEM and scanning transmission electron microscopy (STEM) methods. The TEM and STEM images were taken using a transmission electron microscope STEM TITAN 80-300 by FEI company, fitted with an electron gun with Field

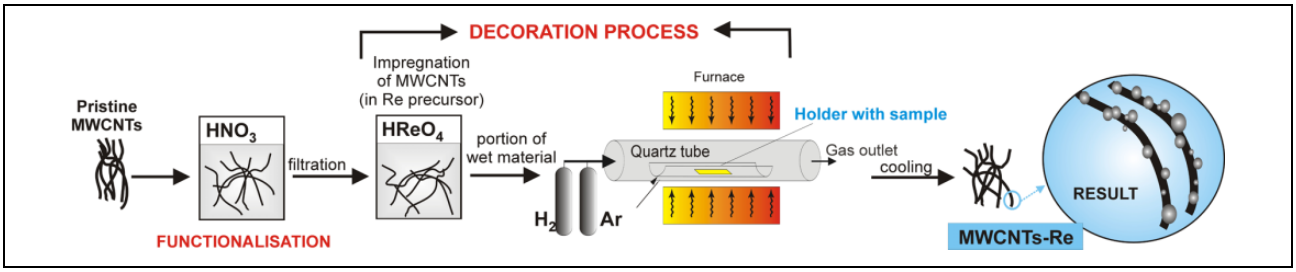

Figure 1. Formation stages of carbon nanotubes decorated with Re nanoparticles. Re: rhenium.

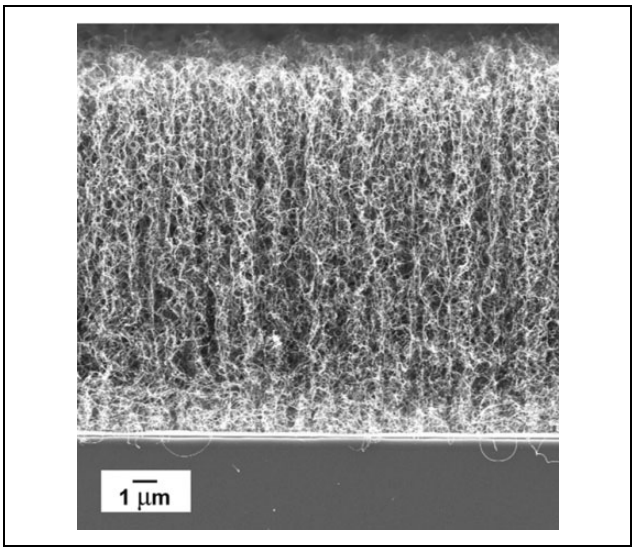

Figure 2. SEM image of as-prepared carbon nanotubes on silicon substrate. SEM: scanning electron microscopy.

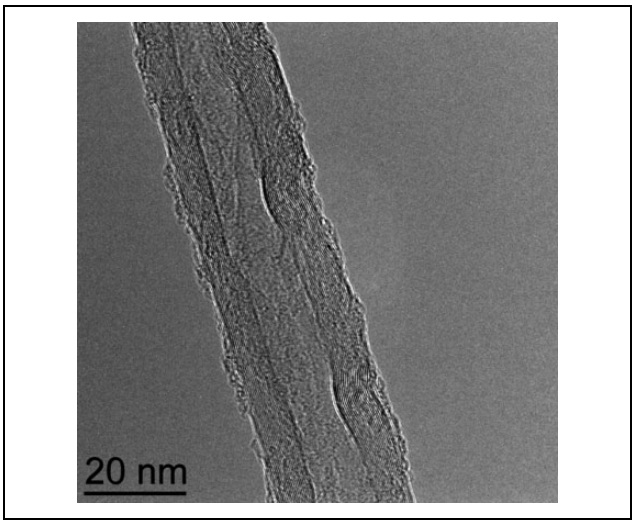

Figure 3. TEM observations of MWCNTs after oxidization intended for further experiments in bright field. TEM: transmission electron microscopy; MWCNT: multiwalled carbon nanotube.

Emission Gun (FEG) field emission, a condenser spherical aberration corrector, STEM scanning system, bright and dark-field detectors and high angle annular dark field. X-ray diffraction measurements were recorded on a Rigaku Denki D/MAX Rapid II diffractometer (cat. no. 2163C104, Rigaku Corporation). The diffractometer is equipped with a rotating silver anode ($\lambda K_\alpha = 0.5608$ Å), an incident beam (002) graphite monochromator and an imaging plate detection system in the Debye-Scherrer geometry.

Results and discussion

The MWCNTs with the diameter of 10–25 nm and the length of 10–30 µm examined under TEM and SEM were used in the course of the experiments. The structure of pristine nanotubes is presented in Figures 2 and 3; it was observed that MWCNTs had small structural defects, and the existence of insignificant amounts of amorphous carbon and individual catalyst particles in the observation field was noticed. The observations carried out under the SEM and TEM allowed to conclude that the investigated pristine CNTs were homogenous within the whole volume of the examined preparation.

Examinations using the Raman spectroscopy method were made to additionally characterize the nanotube material. Raman spectroscopy is considered as an effective tool for the characterization of MWCNTs as it provides information concerning, in particular, material purity. The presence of CNTs in the preparation can be determined according to the distinctive bands occurring on the chart (Figure 4). The D band (approximately 1340 cm^{-1}) informs about the occurrence of structural defects and/or contaminants in the sample. The G band (approximately 1550–1600 cm^{-1}) informs about the degree of order of the graphene structure in the nanotubes. The third visible signal G', also called 2D (defined as an overtone of the D mode), is seen about approximately 2700 cm^{-1}. The following characteristic peaks were located for pristine MWCNTs: D approximately 1345 cm^{-1}, G approximately 1571 cm^{-1} and 2D approximately 2694 cm^{-1} and for a sample containing functionalized MWCNTs, the values are as follows: D approximately 1343 cm^{-1}, G approximately 1571 cm^{-1} and 2D approximately 2695 cm^{-1}. No presence of radial breathing mode (RBM) band was observed during the investigated preparation, which precludes the presence of single-walled nanotubes in the sample. A comparative analysis of the peaks D and G was applied in order to determine the purity of 'as-prepared' CNTs and of the

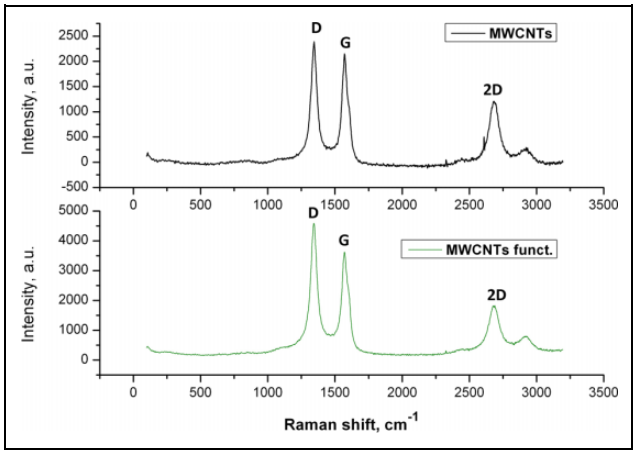

Figure 4. Raman spectrum of pristine and oxidized MWCNTs. MWCNT: multiwalled carbon nanotube.

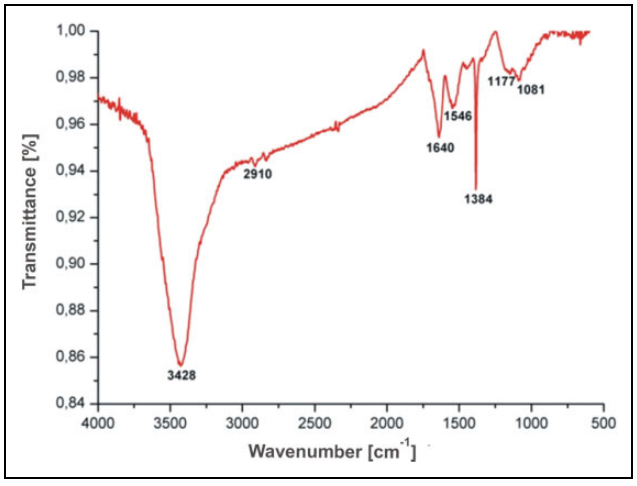

Figure 5. Infrared spectrum of oxidized MWCNTs dedicated to further experiments. MWCNT: multiwalled carbon nanotube.

material oxidized in HNO_3. Following the oxidization process of MWCNTs with HNO_3, the I_D/I_G ratio for a sample undergoing functionalization grows as compared to pristine CNTs. In the analysed cases, I_D/I_G for unmodified MWCNTs is 1.11 whereas the I_D/I_G ratio for the functionalized material is 1.27. It can be claimed, based on the attained outcomes, that oxidation with HNO_3 changed the structure of CNTs by introducing new functional groups onto the surface of MWCNT.

The IR is considered a suitable tool to identify the presence of functional groups attached to the CNTs surface during the oxidization.[38] Figure 5 shows the IR spectra from the MWCNTs dedicated to further experiments which were oxidized using HNO_3. According to Misra et al.[39] who identified weak peak approximately 1445 cm^{-1} as characteristic to MWCNTs, in the presented spectrum, a peak at about 1449 cm^{-1} also occurs. A pronounced peak at approximately 3428 cm^{-1} and peak located at approximately 1640 cm^{-1} are visible on the IR spectra, which are

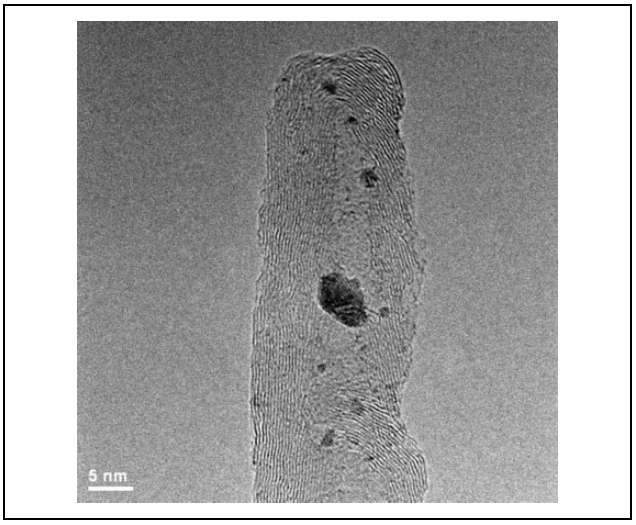

Figure 6. MWCNT-10%Re nanocomposite – TEM observations in bright field. MWCNT: multiwalled carbon nanotube; TEM: transmission electron microscopy; Re: rhenium.

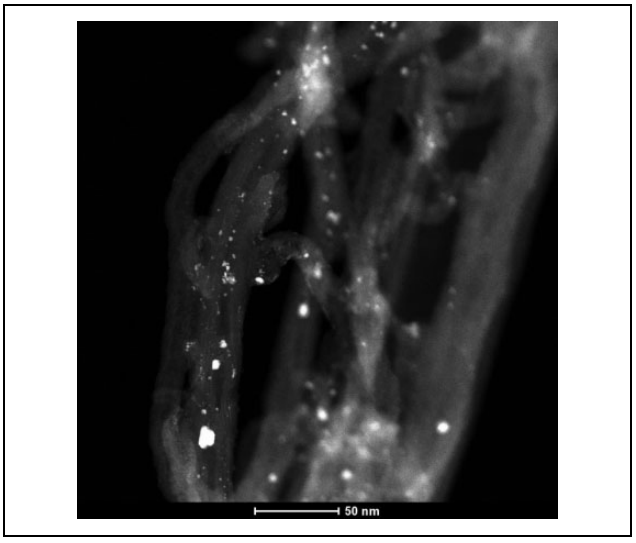

Figure 7. MWCNT-10%Re nanocomposite – STEM observations using HAADF detector in dark field. MWCNT: multiwalled carbon nanotubes; STEM: scanning transmission electron microscopy; HAADF: high angle annular dark field; Re: rhenium.

characteristic for the stretching vibrations of O–H bonds and bending O–H, respectively. This can be a signal from the residual water in the sample or this can be attributed to the oscillation of carboxyl groups adsorbed on the external walls of MWCNTs after HNO_3 treatment.[39,40] A small peak located at approximately 1081 cm^{-1} can be ascribed as signal from C–O stretching groups. The existence of a peak at approximately 1384 cm^{-1} is related to the presence of some nitrate impurities.

The images of CNTs decorated with a weight percentage of Re nanoparticles of, respectively, 10%, 20% and 30% are shown in Figures 6 to 11. The TEM examinations have shown that the materials received differ significantly in

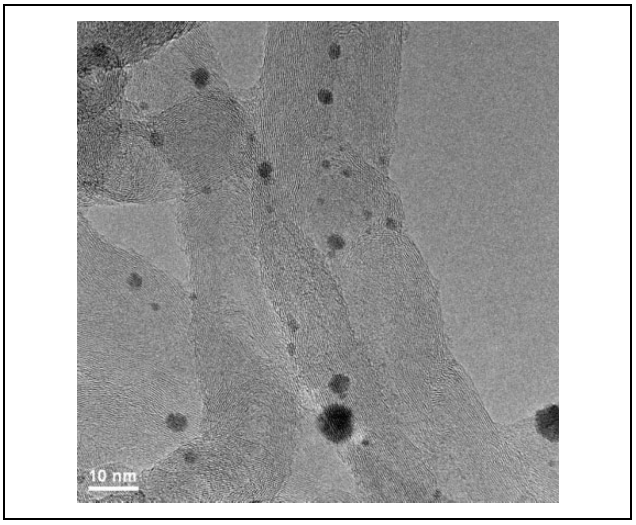

Figure 8. MWCNT-20%Re nanocomposites – TEM observations in bright field. MWCNT: multiwalled carbon nanotubes; TEM: transmission electron microscopy; Re: rhenium.

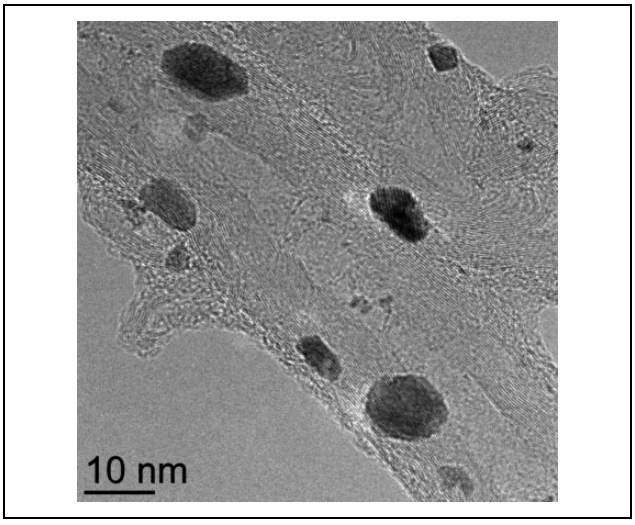

Figure 10. MWCNT-30%Re nanocomposites – TEM observations in bright field. MWCNT: multiwalled carbon nanotubes; STEM: scanning transmission electron microscopy; Re: rhenium.

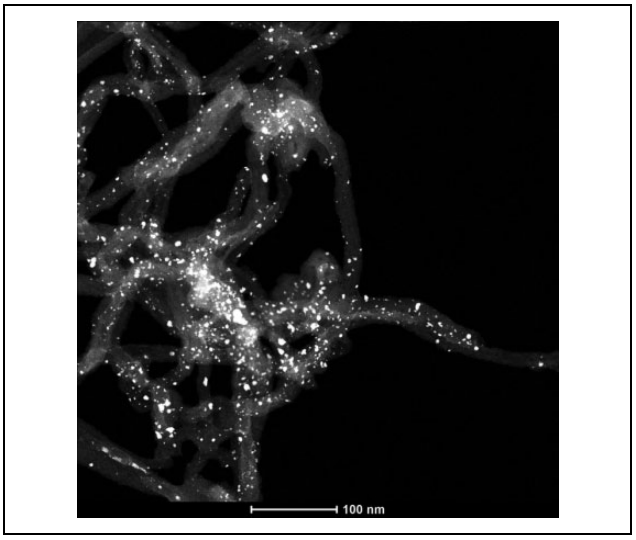

Figure 9. MWCNT-20%Re nanocomposites – STEM observations using HAADF detector in dark field. MWCNT: multiwalled carbon nanotube; STEM: scanning transmission electron microscopy; HAADF: high angle annular dark field; Re: rhenium.

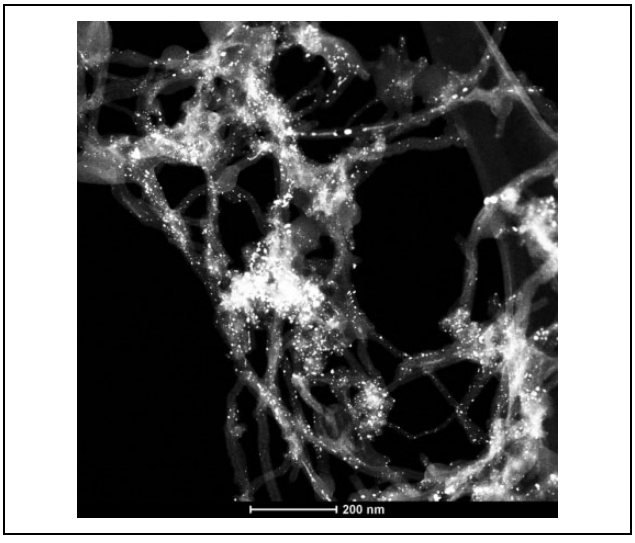

Figure 11. MWCNT-30%Re nanocomposites – STEM observations using HAADF detector in dark field. MWCNT: multiwalled carbon nanotubes; STEM: scanning transmission electron microscopy; HAADF: high angle annular dark field; Re: rhenium.

terms of structure. It can be concluded by considering an MWCNTS-Re nanocomposite with 10% fraction of Re (Figures 6 and 7) that the material is not homogenous within its whole volume. The Re nanoparticles are deposited on the external walls of CNTs, and Re nanoparticles situated inside the core of MWCNTs are also discernible. The diameter of such nanoparticles differs largely. The nanoparticles fabricated, as compared to nanocomposites produced by chemical synthesis method,[41,42] are relatively larger. Visually, a nanocomposite containing 10% of Re has a small number of nanoparticles in the field of observation. Uncoated nanotubes were also discovered during microscope investigations, which may signify that nanotubes are dispergated unevenly in a medium containing Re. Figures 8 and 9 present the results of microscopic observations of a nanocomposite consisting of CNTs with a Re nanoparticle content of 20% in weight. The Re nanoparticles are arranged quite evenly across the entire surface of CNTs. A nanotube material with 20% of Re weight percentage exhibits the first symptoms of nanoparticles agglomeration, whereas the decisively biggest clusters are well discernible on the photos of MWCNTs-Re nanocomposite with a Re content of 30% in weight (Figures 10 and 11). The nanocomposite with the Re content of 20% shows the highest homogeneity considering the nanomaterials presented. The microscopic observations carried out using

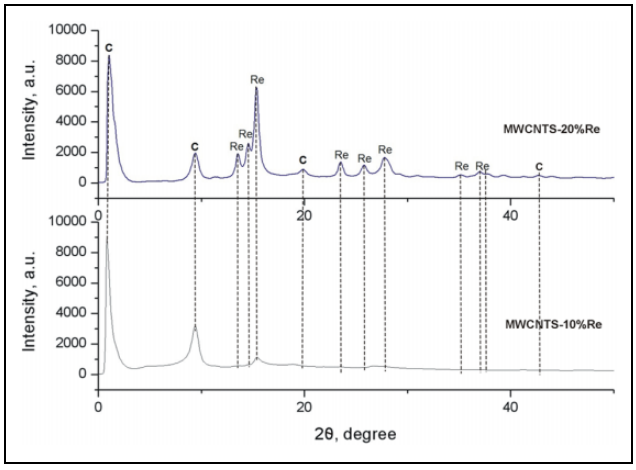

Figure 12. XRD spectra related to MWCNTs-Re samples with Re weight percentage of 10% and 20%. XRD: X-ray diffraction; MWCNT: multiwalled carbon nanotube; Re: rhenium.

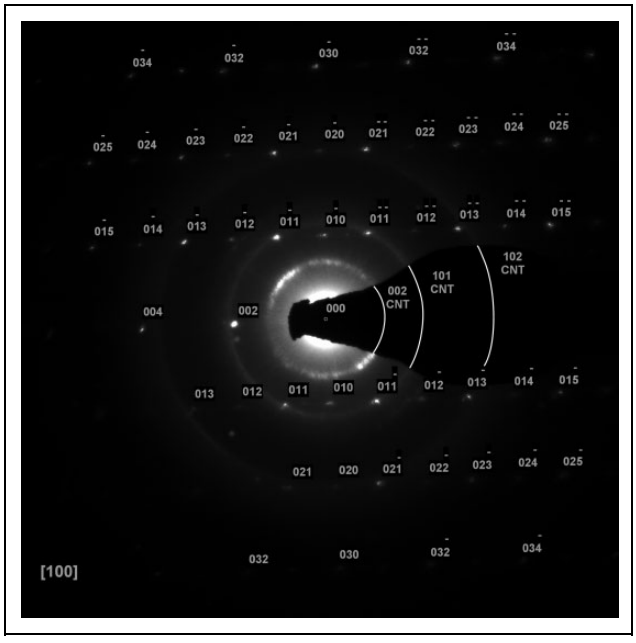

Figure 13. Diffraction pattern corresponding to carbon nanotubes decorated with Re nanocrystals. Re: rhenium.

a TEM clearly demonstrate that the growth of Re nanoparticles content on the surface of CNTs is associated with a growing tendency of their agglomeration.

Figure 12 presents the results of an X-ray diffraction (XRD) phase analysis of CNTs containing 10% and 20% of Re nanoparticles by mass, confirming the chemical composition of the samples. The powder samples were measured in glass capillaries with the diameter of 1.5 mm and the wall thickness of 0.01 mm. The collimated beam width of the sample was 0.3 mm. In order to remove the background, additional measurements were carried out for the empty capillary and the background signal was then subtracted from the intensities recorded for the samples. Rigaku/XRD software (version 2.3.3, cat. no. 2163C202, Rigaku Corporation), which is a comprehensive package controlling a video image of the sample, data collection and X-ray image processing, was used for the reduction of 2D diffraction patterns to 1D functions of intensity versus the scattering angle. It is also indicated by analysing the diffraction pattern that the intensity of the registered peaks is growing as the fraction of Re nanoparticles is increasing. The material was identified by comparing the observed reflexes with a diffraction pattern of CNTs and Re available from The International Centre for Diffraction Data (ICDD) (file no. 01-1231) possessing information concerning the situation of diffraction lines and their relative intensity. The recorded peaks corresponding to reflexes coming from the Re planes are as follows: 14.5° (Miller's indicators: 002); 15.3° (101); 23.4° (110); 25.7° (103); 28.2° (201); 35.1° (203); 37.2° (211); 37.6° (114).

The phase composition of the studied material was confirmed also by using the results of electron diffraction. A diffraction image of a material containing Re nanoparticles deposited on the surface of CNTs is presented in Figure 13. The presence of distinctive, fuzzy, circular diffraction maximums corresponding to the interplanar distance of (002), (100) and (102) of CNTs with a graphene structure and local reflexes, whose arrangement satisfies the dependencies applicable to distance and interplanar angles of Re with an A3 crystalline structure, was particularly recorded in the course of the investigations using a TEM.

Conclusions

The authors of the publications are interested in nanostructured materials formed by the deposition of metal nanoparticles onto the surface of MWCNTs, including Re, due to an expected synergy of unique physiochemical properties of nanocomposite components, namely, a large specific surface area, high electric conductivity and high chemical and thermal resistance.[29,43] The following aspects of the presented fabrication process are essential: the correctly conducted oxidation and decoration phases, including in particular the accurate dispersion of CNTs in the medium, and an accurately selected chemical composition. The structure of such nanocomposites is dependent upon the weight percentage of Re nanoparticles and their uniform dispersion across the surface of MWCNTs. It was observed that the materials are not homogenous in the entire volume, which is the objective of further optimization efforts. The specificity of the fabrication process prevents the use of mechanical assistance for heating, hence the Re particles exhibit an agglomeration tendency, especially when Re content in the sample is nearly 30%. Research and development works have concluded that, in case of MWCNTs-Re nanocomposites, the favourable Re rate is between 10% and 20% by mass, which is observable in the photos made using STEM and TEM. The presented MWCNTs-Re fabrication method is effective and universal. Therefore, it is

elaborated other interesting nanocomposites consisting of nanostructured Re combined with carbon nanomaterials, such as single- and double-walled nanotubes and single-walled carbon nanohorns.[44,45]

Declaration of conflicting interests

The author(s) declared no potential conflicts of interest with respect to the research, authorship, and/or publication of this article.

Funding

The author(s) disclosed receipt of the following financial support for the research, authorship, and/or publication of this article: The article was financed from a statutory grant of the Faculty of Mechanical Engineering of the Silesian University of Technology, Gliwice, Poland in 2016 in the framework of BK/RMT0/2016 project.

References

1. Iijima S. Helical microtubules of graphitic carbon. *Nature* 1991; 354: 56–58. DOI: 10.1038/354056a0.
2. Ebbesen TW. Cones and tubes: geometry in the chemistry of carbon. *Acc Chem Res* 1998; 31: 558–566. DOI: 10.1021/ar960168i.
3. Odom TW, Huang JL, Kim P, et al. Atomic structure and electronic properties of single-walled carbon nanotubes. *Nature* 1998; 391: 62–64. DOI: 10.1038/34145.
4. Kateb B, Yamamoto V, Alizadeh D, et al. Multi-walled carbon nanotube (MWCNT) synthesis, preparation, labeling, and functionalization. *Methods Mol Biol* 2010; 651: 307–317. DOI: 10.1007/978-1-60761-786-0_18.
5. Wang M, Qiu X and Zhang X. Mechanical properties of super honeycomb structures based on carbon nanotubes. *Nanotechnology* 2007; 18(7): 075711. DOI: 10.1088/0957-4484/18/7/075711.
6. Dobrzańska-Danikiewicz Foresight of material surface engineering as a tool building a knowledge based economy. *Mater Sci Forum* 2012; 706–709: 2511–2516. DOI: 10.4028/www.scientific.net/ MSF.706-709.2511.
7. Avouris P, Chen Z and Perebeinos V. Carbon-based electronics. *Nature Nanotechnol* 2007; 2: 605–615. DOI: 10.1038/nnano.2007.300.
8. He H, Pham-Huy LA, Dramou P, et al. Carbon nanotubes: applications in pharmacy and medicine. *BioMed Res Int* 2013; 2013: 1–12/578290. DOI: 10.1155/2013/578290.
9. Usui Y, Haniu H, Tsuruoka S, et al. Carbon nanotubes innovate on medical technology. *Med Chem* 2012; 2(1): 1–6. DOI: 10.4172/2161-0444.1000105.
10. Nabiałek M, Pietrusiewicz P, Dośpiał M, et al. Influence of the cooling speed on the soft magnetic and mechanical properties of Fe61Co10Y8W1B20 amorphous alloy. *J Alloys Compd* 2014; 615(Suppl 1): S56–S60. DOI: 10.1016/j.jallcom.2013.12.236.
11. Kima U, Pcioneka R, Aslama DM, et al. Synthesis of high-density carbon nanotube films by microwave plasma chemical vapor deposition. *Diam Relat Mater* 2001; 10(11): 1947–1951. DOI: 10.1016/S0925-9635(01)00384-3.
12. Poncharal P, Wang ZL, Ugarte D, et al. Electrostatic deflections and electromechanical resonances of carbon nanotubes. *Science* 1999; 283: 1513–1516. DOI: 10.1126/science.283.5407.1513.
13. Bellucci S. Carbon nanotubes: physics and applications. *Phys C* 2005; 2(1): 34–47. DOI: 10.1002/pssc.200460105.
14. Dobrzańska-Danikiewicz A. The acceptation of the production orders for the realisation in the manufacturing assembly systems. *J Mater Proc Technol* 2006; 175: 123–132. DOI: 10.1016/j.jmatprotec.2005.04.001.
15. Krenczyk D and Dobrzańska-Danikiewicz A. The deadlocks protection method used in the production systems. *J Mater Proc Technol* 2005; 164–165: 1388–1394. DOI: 10.1016/j.jmatprotec.2005.02.056.
16. Star A, Joshi V, Skarupo S, et al. Gas sensor array based on metal-decorated carbon nanotubes. *J Phys Chem B* 2006; 110(42): 21014–21020. DOI: 10.1021/jp064371z.
17. Lu Y, Li J, Han J, et al. Room temperature methane detection using palladium loaded single-walled carbon nanotube sensors. *Chem Phy Lett* 2004; 391(4–6): 344–348. DOI: 10.1016/j.cplett.2004.05.029.
18. Li L and Xing Y. Pt−Ru nanoparticles supported on carbon nanotubes as methanol fuel cell catalysts. *J Phys Chem C* 2007; 111(6): 2803–2808. DOI: 10.1021/jp0655470.
19. Saminathan K, Kamavaram V, Veedu V, et al. Preparation and evaluation of electrodeposited platinum nanoparticles on in situ carbon nanotubes grown carbon paper for proton exchange membrane fuel cells. *Int J Hydrogen Energy* 2009; 34(9): 3838–3844. DOI: 10.1016/j.ijhydene.2009.03.009.
20. Ajayan PM and Zhou OZ. Applications of Carbon Nanotubes. In: Dresselhaus MS, Dresselhaus G and Avouris P (eds) *Carbon Nanotubes: Synthesis, Structure, Properties, and Applications*. New York: Springer Verlag Berlin Heidelberg, 2001, pp. 391–425. DOI: 3-540-41o86-4.
21. Jingyu S, Jianshu H, Yanxia C, et al. Hydrothermal synthesis of Pt-Ru/MWCNTs and its electrocatalytic properties for oxidation of methanol. *Int J Elect Sci* 2007; 2: 64–71.
22. Hampel CA. *Rare metals handbook*. 2nd ed. London: Reinhold Publishing Corporation, 1961. p. 715.
23. Polyak DE. 2012 *Minerals Yearbook. Rhenium [Advance Release]*. Virginia: United State Geological Survey, 2012. 62.1–62.5.
24. Philippe L, Peyrot I, Michler J, et al. Yield stress of monocrystalline rhenium nanowires. *Appl Phys Lett* 2007; 91: 111919. DOI: 10.1063/1.2785153.
25. Wrona A, Staszewski M, Czepelak M, et al. Properties of rhenium-based master alloys prepared by powder metallurgy techniques. *Arch Mater Sci Eng* 2010; 45(2): 95–101.
26. Vučina JL and Han Ruben SR. Production and therapeutic application of rhenium isotopes, rhenium-186 and rhenium-188: Radioactive pharmaceuticals of the future. *Med Preg* 2003; 56(7–8): 362. DOI: 10.2298/MPNS0308362V.
27. Burch R. The oxidation state of rhenium and its role in rhenium-platinium reforming catalysts. *Plat Meter Rev* 1978; 22(2): 57–60.

28. Dobrzańska-Danikiewicz AD, Wolany W, Benke G, et al. The new MWCNTs-rhenium nanocomposite. *Physics B* 2014; 251(12): 2485–2490. DOI: 10.1002/pssb.201451360.
29. Dobrzańska-Danikiewicz AD, Cichocki D, Pawlyta M, et al. Synthesis conditions of carbon nanotubes with the chemical vapor deposition method. *Physics B* 2014; 251(12): 2420–2425. DOI: 10.1002/pssb.201451178.
30. Dobrzańska-Danikiewicz AD, Cichocki D, Łukowiec D, et al. Carbon nanotubes synthesis time versus their layer height. *Arch Mater Sci Eng* 2014; 69(1): 1–5.
31. Rosca ID, Watari F, Uo M, et al. Oxidation of multiwalled carbon nanotubes by nitric acid. *Carbon* 2005; 43(15): 3124–3131. DOI: 10.1016/j.carbon.2005.06.019.
32. Puech P, Hu T, Sapelkin A, et al. Charge transfer between carbon nanotubes and sulfuric acid as determined by Raman spectroscopy. *Phys Rev B* 2012; 85(20): 205412. DOI: http://dx.doi.org/10.1103/PhysRevB.85.205412.
33. Blanchard NP, Hatton RA and Silva SRP. Tuning the work function of surface oxidized multi-wall carbon nanotubes via cation exchange. *Chem Phys Lett* 2007; 434: 92–95. DOI: 10.1016/j.cplett.2006.11.100.
34. Osorio AG, Silveira ICL, Bueno VL, et al. H2SO4/HNO3/HCl-Functionalization and its effect on dispersion of carbon nanotubes in aqueous media. *Appl Surf Sci* 2008; 255(5): 2485–2489. DOI: 10.1016/j.apsusc.2008.07.144.
35. Thandavan TMK, Wong CS, Gani SMA, et al. [O][H] functionalization on carbon nanotube using (O2–H2) gasmixture DC glow discharge. *Appl Nanosci* 2012; 2(1): 47–53. DOI: 10.1007/s13204-011-0040-1.
36. Peng Y and Liu H. Effects of oxidation by hydrogen peroxide on the structures of multiwalled carbon nanotubes. *Ind Eng Chem Res* 2006; 45(19): 6483–6488. DOI: 10.1021/ie0604627.
37. Park KC, Hayashi T, Tomiyasu H, et al. Progressive and invasive functionalization of carbon nanotube sidewalls by diluted nitric acid under supercritical conditions. *J Mater Chem* 2005; 15(3): 407–411. DOI: 10.1039/B411221K.
38. Lehman JH, Terrones M, Mansfield E, et al. Evaluating the characteristics of multiwall carbon. *Carbon* 2011; 49(8): 2581–2602. DOI: 10.1016/j.carbon.2011.03.028.
39. Misra A, Tyagi PK, Rai P, et al. FTIR spectroscopy of multiwalled carbon nanotub es: a simple ap proach to study the nitroge n doping. *J Nanosci Nanotechnol* 2007; 7(6): 1820–1823. DOI: 10.1166/jnn.2007.723.
40. Lima G, Midori De Oliveira F, Ohara M, et al. Evaluation of Histidine Functionalized Multiwalled Carbon Nanotubes for Improvement in the Sensitivity of Cadmium Ions Determination in Flow Analysis. In: Bianco S (ed) *Carbon Nanotubes - From Research to Applications*. Rijeka, Croatia: InTech, 2011, pp. 67–80. DOI: 10.5772/17811.
41. Dobrzańska-Danikiewicz AD and Łukowiec D. Synthesis and characterisation of Pt/MWCNTs nanocomposites. *Phys B* 2013; 250(12): 2569–2574. DOI: 10.1002/pssb.201300083.
42. Boneta F, Delmasa V, Grugeona S, et al. Synthesis of monodisperse Au, Pt, Pd, Ru and Ir nanoparticles in ethylene glycol. *Nanostruct Mater* 1999; 11(8): 1277–1284. DOI: 10.1016/S0965-9773(99)00419-5.
43. Dobrzańska-Danikiewicz A, Łukowiec D, Pawlyta M, et al. Resistance changes of carbon nanotubes decorated with platinum nanoparticles in the presence of hydrogen at different and constant concentrations. *Phys B* 2014; 251(12): 2426–2431. DOI: 10.1002/pssb.201451179.
44. Wolany W. *The newly developed nanocomposites consisting of nanostructured rhenium combined with carbon nanomaterials*. Poland: Gliwice, 2016, p. 262.
45. Dobrzańska-Danikiewicz AD and Wolany W. A rhenium review – from discovery to novel applications. *Arch Mater Sci Eng* 2016; 82(2): 70–78.